



Cite this: *Biomater. Sci.*, 2018, **6**, 2932

## Self-healing, stretchable and robust interpenetrating network hydrogels†

Laura J. Macdougall,<sup>a</sup> Maria M. Pérez-Madrugal,<sup>b</sup> Joshua E. Shaw,<sup>c</sup> Maria Inam,<sup>a</sup> Judith A. Hoyland,<sup>b,c,d</sup> Rachel O'Reilly,<sup>b</sup> Stephen M. Richardson<sup>b,c</sup> and Andrew P. Dove<sup>b,\*</sup>

A self-healable stretchable hydrogel system that can be readily synthesized while also possessing robust compressive strength has immense potential for regenerative medicine. Herein, we have explored the addition of commercially available unfunctionalized polysaccharides as a route to synthesize self-healing, stretchable poly(ethylene glycol) (PEG) interpenetrating networks (IPNs) as extracellular matrix (ECM) mimics. The introduction of self-healing and stretchable properties has been achieved while maintaining the robust mechanical strength of the original, single network PEG-only hydrogels (ultimate compressive stress up to 2.4 MPa). This has been accomplished without the need for complicated and expensive functionalization of the natural polymers, enhancing the translational applicability of these new biomaterials.

Received 25th July 2018,  
Accepted 9th September 2018

DOI: 10.1039/c8bm00872h

rsc.li/biomaterials-science

For hydrogels to be competitive candidates against current commercial biomaterials, they need to be prepared by straightforward synthetic routes using commercially available precursors to ensure that they are both translatable and cost effective.<sup>1–5</sup> Recently, hydrogels have attracted a huge interest in the biomedical field because of their ability to mimic the features of the native extracellular matrix (ECM) (*i.e.* porous structure, adequate stiffness and controlled mechanical properties) which allows cell growth and proliferation to be studied *in vitro*.<sup>6–8</sup> However, to improve their properties further, the design of hydrogels should also target other requirements, which include: (i) gelation *in situ* at the defect site (*i.e.* injectability), (ii) self-healing, and (iii) enhanced mechanical properties.<sup>9,10</sup>

Click chemistry approaches,<sup>11</sup> which have been used for many years for hydrogel synthesis,<sup>12,13</sup> not only enable the formation of hydrogels through highly efficient reactions using easily accessible functional groups (no need for purification steps),<sup>14–16</sup> but also allow for tunable control of hydrogel properties. For instance, robust poly(ethylene glycol) (PEG) hydro-

gels prepared using the nucleophilic thiol-yne addition reaction, which has been recently reported by our group<sup>17–19</sup> and others,<sup>20,21</sup> formed in phosphate buffered saline (PBS) solution without the need for an external catalyst. By simply functionalizing commercially available PEG precursors, we feasibly obtained synthetic *in situ* forming hydrogels in an efficient manner, thus fulfilling one of the above requirements. These thiol-yne hydrogels display excellent mechanical properties (compressive stress under repeated compression up to 2.4 MPa), as well as tunable, non-swelling, and cytocompatible characteristics. However, there are still areas to address (*e.g.* stretchability and self-healing properties) before they can become competitive candidates as new biomaterials.

Nature provides us with a wide range of biocompatible natural polymers (*e.g.* alginate and gelatin) that are cheap to produce and can easily form hydrogels with good self-healing and tensile properties.<sup>22–24</sup> While widely studied as the basis for constructing hydrogel materials, they cannot be tuned to different biological environments, display weak compressive strengths<sup>25–27</sup> and can lack reproducible properties,<sup>28,29</sup> which limits their potential for advanced hydrogel engineering. To overcome the drawbacks of individual networks, interpenetrating networks (IPNs) can be designed.<sup>30–32</sup> IPNs are formed through intertwining two hydrogel networks together (*e.g.* a natural and a synthetic hydrogel system) during gelation, which enables the resultant IPN to synergistically display the benefits from both systems.<sup>33–35</sup> We hypothesized that blending a natural polymer hydrogel with the robust synthetic thiol-yne PEG hydrogel system would result in a thiol-yne IPNs that possess the advantages of both the natural hydrogel system

<sup>a</sup>Department of Chemistry, University of Warwick, Coventry, CV4 7AL, UK

<sup>b</sup>School of Chemistry, University of Birmingham, Edgbaston, Birmingham, B15 2TT, UK. E-mail: a.dove@bham.ac.uk

<sup>c</sup>Division of Cell Matrix Biology and Regenerative Medicine, School of Biological Sciences, Faculty of Biology, Medicine and Health, Manchester Academic Health Science Centre, University of Manchester, Manchester M13 9PL, UK

<sup>d</sup>NIHR Manchester Biomedical Research Centre, Central Manchester Foundation Trust, Manchester Academic Health Science Centre, Manchester, UK

†Electronic supplementary information (ESI) available. See DOI: 10.1039/c8bm00872h



(*i.e.* self-healing and stretchability) and the synthetic system (*i.e.* tunable stiffness, reproducibility, and robust compressive strength), which are ideal characteristics of an ECM mimic.

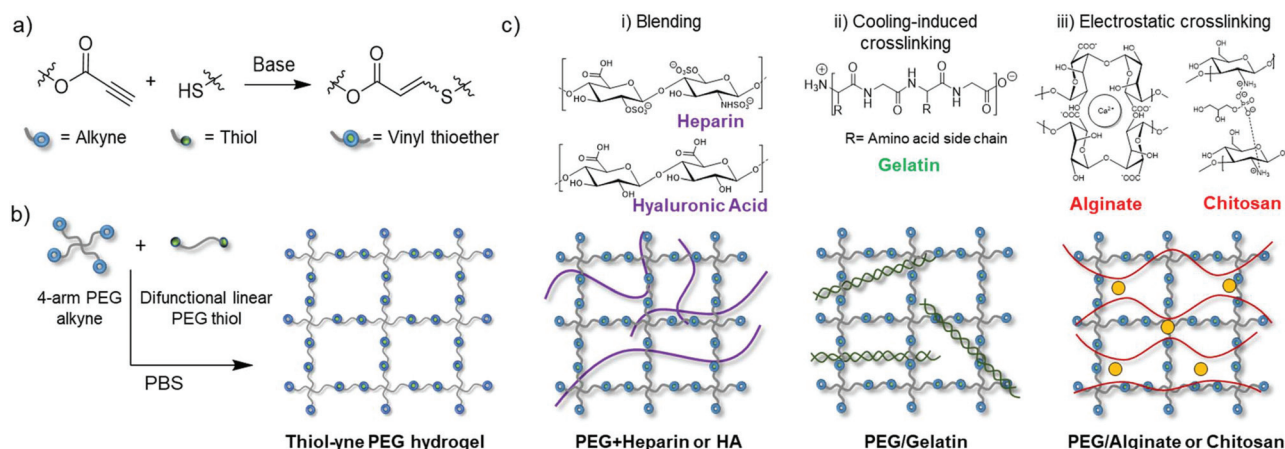
To investigate the IPN strategy, five commercially available unfunctionalized natural polymers (*i.e.* alginate, chitosan, gelatin, heparin, or hyaluronic acid (HA)) were blended within the thiol–yne hydrogel system, which was comprised from 4-arm PEG alkyne ( $2 \text{ kg mol}^{-1}$ ) and difunctional linear PEG thiol ( $4 \text{ kg mol}^{-1}$ ) precursors (Scheme 1).<sup>17</sup> The tensile, self-healing and other mechanical properties were subsequently characterized. Hydrogels were formed in PBS solution (pH 7.4) in a 1:1 ratio of alkyne:thiol end groups at 8 wt% PEG content (hereafter referred as PEG-only hydrogels). The hydrogels formed within 3 min owing to the high efficiency and fast reaction rate of the nucleophilic thiol–yne click reaction and were used without further purification. Alginate and chitosan were incorporated into the thiol–yne network as a secondary loose electrostatic network crosslinked with either  $\text{CaCO}_3/\text{D-}(+)\text{-glucono-1,5-lactone}$  (GDL) or glycerol phosphate (GP), respectively (Scheme 1). Gelatin was heated to  $70 \text{ }^\circ\text{C}$  before mixing with the PEG alkyne precursor to allow for the reorganization of the peptide chains to form a secondary electrostatic network through tertiary coils. These systems were named accordingly to reflect the formation of a secondary electrostatic gel formation: PEG/natural polymer (alginate, chitosan or gelatin) IPNs. HA and heparin were added to the single thiol–yne PEG network to evaluate the addition of an uncrosslinked single natural polymer to the thiol–yne hydrogel in the absence of IPN formation. This was reflected in the naming system using ‘+’ to signify the natural polymer was only blended (*i.e.* not crosslinked) within the thiol–yne PEG hydrogel; PEG + natural polymer (HA or heparin), (Scheme 1).

To create thiol–yne IPNs with superior properties, the required amounts of PEG and natural polymer were optimized to ensure that (i) all the polysaccharides were homogeneously

distributed within the dense thiol–yne hydrogel network, avoiding phase separation, and (ii) the resulting IPN benefitted from the advantages of all the components (Table S1, Fig. S1 and S2†). Hence, through this optimization process, it was determined that all the thiol–yne natural polymer systems would be synthesized with 8 wt% thiol–yne PEG and 1 wt% natural polymer content (overall 9 wt% solid content, Scheme 1). Additionally, to ensure that the final IPN systems were homogenous, all the components were thoroughly mixed during hydrogel preparation (*i.e.* PEG alkyne and the natural polymer were dissolved in PBS and then mixed with PEG thiol dissolved in PBS with/without counterion, Scheme S1†). As a result, transparent hydrogels were formed within 10 min, and their swelling, degradation profiles and mesh size were fully characterized (Fig. S3–S5†).

Synthesizing hydrogels with good tensile properties allows them to withstand the surrounding pressure of a biological environment, thus better mimicking the behavior of soft tissue.<sup>36</sup> It is important that the robust compressive strength of the original thiol–yne hydrogels ( $2 \pm 0.5 \text{ MPa}$ ) is maintained to withstand external compressive pressure. To verify that our IPNs fulfill such a requirement, the compressive stress of the thiol–yne IPNs was attained by uniaxial compression testing; hydrogels were made in cylindrical molds and subjected to strains up to 98% while the resultant stress was recorded.

Indeed, PEG/Alginate and PEG/Gelatin systems showed high compressive strengths ( $2.3 \pm 0.4 \text{ MPa}$  and  $2.4 \pm 0.1 \text{ MPa}$ , respectively, Fig. 1a), which demonstrates the robust nature of the IPNs working together to form biomaterials for high load bearing environments (*e.g.* articular cartilage joints). However, the compressive strength of the hydrogels where chitosan, heparin, and HA was incorporated, resulted in weaker materials. The addition of single chains to the thiol–yne network formation, along with the acidic nature of the chitosan solution, reduced the compressive strength to



**Scheme 1** (a) Nucleophilic base-catalyzed thiol–yne reaction; (b) schematic of the dense thiol–yne PEG hydrogel formation (8 wt%) obtained by crosslinking a 4-arm PEG alkyne ( $2 \text{ kg mol}^{-1}$ ) with a difunctional linear PEG thiol ( $4 \text{ kg mol}^{-1}$ ); (c) schematics of the IPN hydrogels prepared by introducing a secondary loose network based on: (i) uncrosslinked natural polymers (*i.e.* heparin or hyaluronic acid); (ii) gelatin displaying a cooling-induced tertiary coiled structure; and (iii) electrostatically crosslinked natural polymers (*i.e.* alginate crosslinked with calcium; chitosan crosslinked with glycerol phosphate).



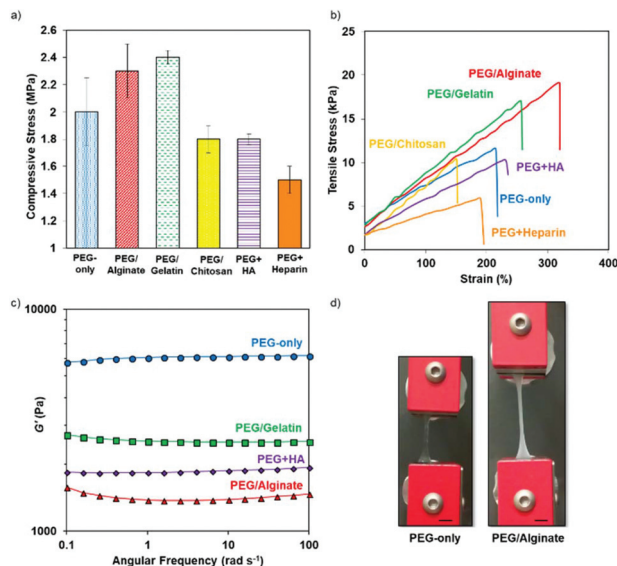


**Fig. 1** (a) Maximum compression stress of the systems at 98% strain; (b) a representative tensile stress/strain graph for each PEG/natural polymer system; (c) a representative frequency sweep for each system at 0.5% strain for the systems with improved tensile properties (see ESI† for all systems); (d) picture of the tensile testing of PEG-only and PEG/Alginate systems showing the increased tensile properties of the PEG/Alginate system, scale bar = 1 cm.

1.5–1.8 MPa. Nevertheless, these systems still provided sufficient support as cell culture scaffolds with a similar strength to articular cartilage ECM (1.5 MPa).<sup>37</sup>

For tensile testing, the samples were formed in dog bone molds, left to cure, and then subjected to uniaxial tensile testing. The PEG-only system was able to withstand a strain of  $204 \pm 42\%$ , which is comparable to that displayed by PEG systems prepared using radical thiol-ene chemistry, which typically reaches a strain of 150%.<sup>38,39</sup> More remarkably, the thiol-ene IPN hydrogels with alginate and gelatin displayed improved tensile properties, reaching strain values up to  $353 \pm 36\%$  (Fig. 1b). This increase in tensile performance demonstrates a facile way of improving the properties of these hydrogels by simply introducing a secondary electrostatic loose network that can complement the efficient nucleophilic thiol-ene cross-linking chemistry used. Interestingly, the strain at break for the PEG/Alginate IPN can be further enhanced (up to  $490 \pm 88\%$ , Fig. S6†) by increasing the  $\text{Ca}^{2+}$  ion content although this impacts the strength of the hydrogel and results in opaque hydrogels, which could make imaging encapsulated cells more difficult. In contrast, incorporating a single natural polymer (HA or heparin) into the thiol-ene hydrogels gave no significant improvement to the tensile performance ( $260 \pm 49\%$  and  $168 \pm 58\%$ , respectively). In this case, the single natural polymers disrupted the thiol-ene crosslinking reaction as indicated by gel fraction (GF) and mesh size calculations. GF values decreased from 75% for PEG-only to 32 and 56% for HA and heparin, respectively, while mesh size increased from 10.9 nm to 13.6 and 12.4 nm, respectively (Fig. S3†),

which indicates that the networks had more defects and dangling ends. Finally, as chitosan is only soluble in acidic conditions, the overall pH of the system was lowered during the hydrogel preparation, which affected the efficiency of nucleophilic thiol-ene reaction (characterized again by a decrease in GF from 75 to 55%, Fig. S3†). As a result, the PEG/Chitosan system exhibited inferior properties, including a lower strain at break ( $158 \pm 58\%$ ), than displayed by the PEG-only system.

Through conducting rheological studies, the reason for such improved tensile performance was revealed, in particular for the PEG/Alginate system. The single covalent network (PEG-only) is a moderately stiff system ( $G' = 5.5 \pm 0.5$  kPa); however, by incorporating a natural polymer to form an IPN,  $G'$  decreases to  $1.4 \pm 0.03$  kPa. This allows the material to become softer and have the ability to withstand higher amounts of strain (Fig. 1c and S8†), also seen for the PEG/Gelatin system ( $G'$  decreases to  $1.3 \pm 0.5$  kPa). Reducing the stiffness of these materials brings them into the intermediate range for soft biological tissue,<sup>40</sup> opening up an opportunity for these materials to potentially improve cell proliferation and differentiation in an applicable and relevant environment compared to the PEG-only network. This reduction in  $G'$ , combined with the electrostatic interactions between the negatively charged alginate chains and the positive calcium ions in the PEG/Alginate system, allows the hydrogels to show the overall biggest improvement in tensile properties. Even though a larger decrease in  $G'$  is seen for the other networks, this has a negative effect on their ability to withstand external forces and is, therefore, a contributing factor to their poor tensile performance.

Overall, the PEG/Alginate IPN exhibited the most improved tensile performance (Fig. 1d), having the ability to mimic the stretchability of native tissue while maintaining the robust nature of the thiol-ene hydrogels. The hydrogel material benefits from the features of both the dense thiol-ene matrix and the secondary electrostatic crosslinked network, resulting in an ideal material for an ECM mimic.<sup>25</sup>

Material self-healing, which implies spontaneous new bond formation when the original bonds are disrupted, is driven, for instance, by non-covalent interactions (*i.e.* hydrogen bonding, disulfide exchange, metal ligand complexes).<sup>41–43</sup> Thus, a hydrogel that can be easily made and displays high compressive strength but is also a self-healable hydrogel has immense potential for regenerative medicine. Hence, to test the self-healing nature of the strong stretchable thiol-ene materials, dog-bone shaped samples were prepared and left to cure for 1 h before cutting. The cut pieces were then brought back together and left to heal overnight (Fig. S9†). Samples were then subjected to tensile testing, and their stress/strain curves were compared before and after the self-healing process.

During the healing process, the formation of new electrostatic interactions between the natural polymer and the counterions reformed the hydrogel network, thus rendering PEG/Alginate and PEG/Chitosan IPN hydrogels self-healable (Fig. 2a).<sup>44</sup> In contrast, the addition of a single natural polymer



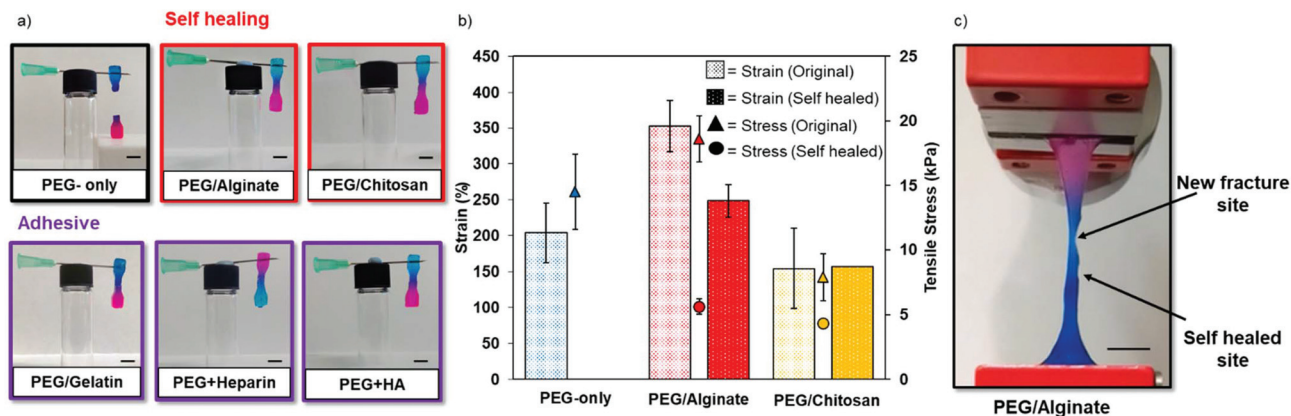


**Fig. 2** Self-healing properties of the PEG/natural polymer hydrogels: (a) pictures of the self-healed/adhesive hydrogels; (b) comparison tensile properties strain (LHS axis, bars) and stress (RHS axis, triangle and circle) of the original and self-healed networks; (c) picture of the tensile properties of the self-healed PEG/Alginate system. Scale bar = 5 mm.

(*i.e.* HA, gelatin, or heparin) did not result in self-healing properties owing to the absence of charged ions to reform electrostatic interactions in the secondary network. These materials were softer but had adhesive properties that allowed them to hold their own weight (Fig. 2a); however, they were unable to self-heal and broke at the cut site when handled (*i.e.* no self-healing had taken place, Video S1†).

To assess the strength of the self-healing networks, PEG/Alginate and PEG/Chitosan self-healed hydrogels were subjected to tensile testing, the failure for both occurring above the healed site, thus indicating that the cut site had fully recovered, and it was not the weakest part of the hydrogel (Fig. 2c). Interestingly, the strain at break for the self-healed PEG/Chitosan IPN was unaffected by the self-healing process, having the ability to recover to the same amount of strain as the original sample (157%, Fig. 2b). The self-healed PEG/Alginate hydrogels broke at a lower tensile stress than the original samples (decreasing from  $353 \pm 36\%$  to  $249 \pm 39\%$ ); however, within the context of hydrogels, they were still able to withstand a large amount of strain (Fig. 2b). A further advantage of this system is the simplicity of the self-healing process (RT, overnight), which allows these materials to easily recover after failure, broadening their applications in a tissue engineering setting. Although the PEG/Chitosan IPN was able to recover their initial tensile properties, the self-healed PEG/Alginate IPN was more robust, as shown by its ability to be twisted, stretched and bent (Fig. 3). Overall, the addition of a secondary electrostatic network to the thiol-yne PEG system resulted in IPNs that presented the best of both systems: robust mechanical properties from the covalent PEG network combined with the high stretchability and self-healing properties of the natural polymer secondary system.

Finally, owing to the improved features acquired through the two hydrogel systems working together (*i.e.* stretchability and self-healing) and their potential for a biological application, the cytotoxicity of PEG/Alginate thiol-yne hydrogels was determined and compared to that displayed by the PEG-

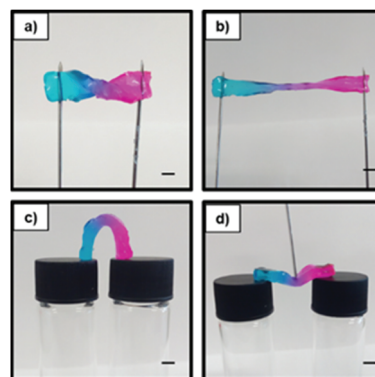


**Fig. 3** Properties of the self-healed PEG/Alginate hydrogels: (a) ability to twist the hydrogel 180°; (b) the twisted hydrogel stretched between two needles; (c) bending properties of the self-healed hydrogels on two vial caps; (d) healed site withstanding the force of localized pressure. Scale bar = 5 mm.

only system, in addition to PEG + HA, where the polysaccharide is only blended (*i.e.* not forming a crosslinked network). Human mesenchymal stem cells (Y201 hTERT-immortalized human clonal MSCs) were encapsulated in a 3D configuration, and cell viability was assessed with alamarBlue® metabolic assay and live-dead fluorescent staining at specific time points (*i.e.* 24, 48, and 72 h, Fig. 4 and S10†). After 24 h of incubation, all hydrogels displayed similar high cell viability, indicating that the thiol-yne matrices are cytocompatible, which is in good agreement with our previous studies.<sup>18,19</sup> Moreover, the incorporation of a polysaccharide within the dense network did not affect cell viability. At longer incubation times (72 h), cell growth was not sustained for the PEG-only system, cell metabolic activity was significantly lower after 72 h in comparison to the 24 h time point, which was not observed for the other two systems. This was also seen by live/dead staining where cell viability decreased significantly ( $88 \pm 3\%$  to  $77 \pm 2\%$  live cells). This was attributed to the difference in how cells



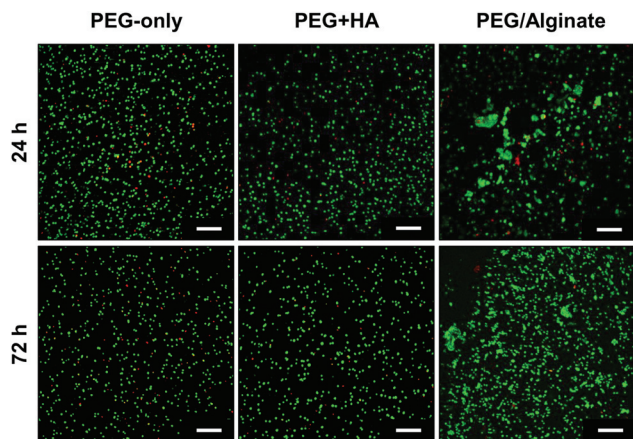


**Fig. 4** Biocompatibility of PEG-only, PEG + HA, and PEG/Alginate click hydrogels. Representative images of 3D encapsulated cells after 24 and 72 h of incubation. Scale bar = 200  $\mu$ m.

distinctively interact with the polymeric matrices and sense their surrounding environment. Features such as the stiffness, porosity, or the presence of charged chains could all attribute to cell metabolic activity.

Remarkably, cell viability after 72 h was significantly higher for PEG/Alginate hydrogels in comparison to the PEG-only hydrogel, viability increased from  $87 \pm 3\%$  to  $95 \pm 2\%$  live cells over a 72 h period. In contrast, no change was observed for PEG + HA ( $92 \pm 2\%/88 \pm 3\%$  live cells). Furthermore, it is important to highlight that cells embedded in the PEG/Alginate hydrogels appeared to aggregate and form clusters, which indicates that in this environment cells move and interact with each other. Hence, PEG/Alginate provided a cytocompatible matrix that supports cell growth. Indeed, by applying a simple and straightforward approach, the PEG/Alginate IPNs possessed enhanced features which resulted in suitable tissue engineering scaffolds.

The excellent features displayed by the addition of a secondary network to the thiol-yne robust networks has demonstrated a simple but effective way to improve the properties of covalent synthetic hydrogel systems. It has highlighted how two systems can work together to produce an advantageous material which possesses the beneficial properties of both systems whilst overcoming the drawbacks of both networks. The addition of alginate chains, crosslinked with calcium ions, has rendered the hydrogels not only stretchable and with enhanced tensile performance, but also with self-healing capabilities. Most importantly, in comparison to the PEG-only system, PEG/Alginate hydrogels exhibit much higher cell viability, suggesting they are ideal matrices for cell growth and proliferation. Our strategy, which is based on exploiting the features of well understood starting materials, still allows hydrogels to be prepared under biological relevant conditions without the need for further purification, and thus can be easily translated to a commercial setting where biomaterials mimicking the ECM are needed.

## Conflicts of interest

There are no conflicts to declare.

## Acknowledgements

EPSRC are thanked for the award of DTP studentships to L. J. M. and M. I. ERC are acknowledged for support to A. P. D. (grant number: 681559) and R. K. O. R. (grant number: 615142). M. M. P.-M. acknowledges funding from the European Union Horizon 2020 research and innovation programme under the Marie Skłodowska-Curie grant agreement no. 703415. BBSRC are thanked for their award of a DTP CASE studentship to J. S. (grant number: BBSRC DTP CASE BB/M011208/1). The Bioimaging Facility microscope used in this study was purchased with grants from BBSRC, Wellcome and the University of Manchester Strategic Fund.

## Notes and references

- 1 E. Caló and V. V. Khutoryanskiy, *Eur. Polym. J.*, 2015, **65**, 252–267.
- 2 K. Y. Lee and D. J. Mooney, *Prog. Polym. Sci.*, 2012, **37**, 106–126.
- 3 A. Bin Imran, K. Esaki, H. Gotoh, T. Seki, K. Ito, Y. Sakai and Y. Takeoka, *Nat. Commun.*, 2014, **5**, 5124.
- 4 S. Mitragotri, P. A. Burke and R. Langer, *Nat. Rev. Drug Discovery*, 2014, **13**, 655–672.
- 5 Y. Lu, A. A. Aimetti, R. Langer and Z. Gu, *Nat. Rev. Mater.*, 2016, **2**, 16075.
- 6 B. V. Slaughter, S. S. Khurshid, O. Z. Fisher, A. Khademhosseini and N. A. Peppas, *Adv. Mater.*, 2009, **21**, 3307–3329.
- 7 M. E. Smithmyer, L. A. Sawicki and A. M. Kloxin, *Biomater. Sci.*, 2014, **2**, 634–650.
- 8 A. M. Rosales and K. S. Anseth, *Nat. Rev. Mater.*, 2016, **1**, 15012.
- 9 C. W. Peak, J. J. Wilker and G. Schmidt, *Colloid Polym. Sci.*, 2013, **291**, 2031–2047.
- 10 Z. Gong, G. Zhang, X. Zeng, J. Li, G. Li, W. Huang, R. Sun and C. Wong, *ACS Appl. Mater. Interfaces*, 2016, **8**, 24030–24037.
- 11 H. C. Kolb, M. G. Finn and K. B. Sharpless, *Angew. Chem., Int. Ed.*, 2001, **40**, 2004–2021.
- 12 K. S. Anseth and H. A. Klok, *Biomacromolecules*, 2016, **17**, 1–3.
- 13 J. E. Moses and A. D. Moorhouse, *Chem. Soc. Rev.*, 2007, **36**, 1249–1262.
- 14 P. M. Kharkar, K. L. Kiick and A. M. Kloxin, *Chem. Soc. Rev.*, 2013, **42**, 7335–7372.
- 15 E. Bakaic, N. M. B. Smeets and T. Hoare, *RSC Adv.*, 2015, **5**, 35469–35486.
- 16 M. A. Azagarsamy and K. S. Anseth, *ACS Macro Lett.*, 2013, **2**, 5–9.



- 17 L. J. Macdougall, V. X. Truong and A. P. Dove, *ACS Macro Lett.*, 2017, **6**, 93–97.
- 18 V. X. Truong, M. P. Ablett, S. M. Richardson, J. A. Hoyland and A. P. Dove, *J. Am. Chem. Soc.*, 2015, **137**, 1618–1622.
- 19 L. J. Macdougall, M. M. Pérez-Madrugal, M. C. Arno and A. P. Dove, *Biomacromolecules*, 2017, **19**, 1378–1388.
- 20 X. Y. Cai, J. Z. Li, N. N. Li, J. C. Chen, E.-T. Kang and L. Q. Xu, *Biomater. Sci.*, 2016, **4**, 1663–1672.
- 21 V. X. Truong, K. M. Tsang and J. S. Forsythe, *Biomacromolecules*, 2017, **18**, 757–766.
- 22 Y. Li, J. Rodrigues and H. Tomas, *Chem. Soc. Rev.*, 2012, **41**, 2193–2221.
- 23 W. Zhao, X. Jin, Y. Cong, Y. Liu and J. Fu, *J. Chem. Technol. Biotechnol.*, 2013, **88**, 327–339.
- 24 T. Coviello, P. Matricardi, C. Marianecchi and F. Alhaique, *J. Controlled Release*, 2007, **119**, 5–24.
- 25 R. DeVolder and H.-J. Kong, *Wiley Interdiscip. Rev.: Syst. Biol. Med.*, 2012, **4**, 351–365.
- 26 S. J. Bidarra, C. C. Barrias and P. L. Granja, *Acta Biomater.*, 2014, **10**, 1646–1662.
- 27 K. Y. Lee and D. J. Mooney, *Chem. Rev.*, 2001, **101**, 1869–1879.
- 28 Y. Wen and J. K. Oh, *Macromol. Rapid Commun.*, 2014, **35**, 1819–1832.
- 29 N. A. Peppas, J. Z. Hilt, A. Khademhosseini and R. Langer, *Adv. Mater.*, 2006, **18**, 1345–1360.
- 30 M. A. Daniele, A. A. Adams, J. Naciri, S. H. North and F. S. Ligler, *Biomaterials*, 2014, **35**, 1845–1856.
- 31 C. Branco da Cunha, D. D. Klumpers, W. A. Li, S. T. Koshy, J. C. Weaver, O. Chaudhuri, P. L. Granja and D. J. Mooney, *Biomaterials*, 2014, **35**, 8927–8936.
- 32 X. Tong and F. Yang, *Biomaterials*, 2014, **35**, 1807–1815.
- 33 I. Liao, F. T. Moutos, B. T. Estes, X. Zhao and F. Guilak, *Adv. Funct. Mater.*, 2013, **23**, 5833–5839.
- 34 E. S. Dragan, *Chem. Eng. J.*, 2014, **243**, 572–590.
- 35 M. Changez, V. Koul, B. Krishna, A. K. Dinda and V. Choudhary, *Biomaterials*, 2004, **25**, 139–146.
- 36 N. Annabi, A. Tamayol, J. A. Uquillas, M. Akbari, L. E. Bertassoni, C. Cha, G. Camci-Unal, M. R. Dokmeci, N. A. Peppas and A. Khademhosseini, *Adv. Mater.*, 2014, **26**, 85–124.
- 37 P. Calvert, *Adv. Mater.*, 2009, **21**, 743–756.
- 38 T. Yang, M. Malkoch and A. Hult, *J. Polym. Sci., Part A: Polym. Chem.*, 2013, **51**, 363–371.
- 39 J. Cui, M. A. Lackey, A. E. Madkour, E. M. Saffer, D. M. Griffin, S. R. Bhatia, A. J. Crosby and G. N. Tew, *Biomacromolecules*, 2012, **13**, 584–588.
- 40 I. Levental, P. C. Georges and P. A. Janmey, *Soft Matter*, 2007, **3**, 299–306.
- 41 A. B. W. Brochu, S. L. Craig and W. M. Reichert, *J. Biomed. Mater. Res., Part A*, 2011, **96**, 492–506.
- 42 A. Pérez-San Vicente, M. Peroglio, M. Ernst, P. Casuso, I. Loinaz, H.-J. Grande, M. Alini, D. Eglin and D. Dupin, *Biomacromolecules*, 2017, **18**, 2360–2370.
- 43 F. R. Kersey, D. M. Loveless and S. L. Craig, *J. R. Soc., Interface*, 2007, **4**, 373–380.
- 44 D. L. Taylor and M. in het Panhuis, *Adv. Mater.*, 2016, **28**, 9060–9093.

